

PALEOSTRESS ANALYSIS OF DEFORMATION-INDUCED MICROSTRUCTURES:

MOINE THRUST ZONE ANJ IKERTOQ SHEAR ZONE

D.L. Kohlstedt and Reid F. Cooper<sup>1</sup>

Maura S. Weathers and John M. Bird<sup>2</sup>

<sup>1</sup>Department of Materials Science and Engineering, Cornell University,  
Ithaca, New York.

<sup>2</sup>Department of Geological Sciences, Cornell University, Ithaca, New York.

## 1. INTRODUCTION

Transmission electron microscopy and transmission optical microscopy observations on experimentally and naturally deformed rocks and minerals have led to the important conclusion that, under the condition of plastic deformation at a constant differential stress, the dislocation density, subgrain size, and grain size are determined by the magnitude of the differential stress (see, for example, Twiss, 1977; Goetze, 1978). The experimentally derived stress-dislocation density, stress-subgrain size, and stress-grain size relations -- here referred to as paleostress scales -- provide a technique of estimating the differential stress appropriate to naturally deformed rocks. It is hoped that this technique will complement the other field and laboratory techniques used to study the deformation history of faults.

The basic question addressed in this paper is "What can we learn about the differential stress level, the deformation conditions, and the deformation mechanisms in deeply eroded fault zones by studying deformation-induced microstructure?"

The organization of this paper is as follows: First, the experimental and theoretical justifications for the differential stress-microstructure relations are outlined. Second, optical and transmission electron microscopy observations on the deformation-induced microstructures are presented for two fault zones, the Moine thrust zone in Scotland and the Ikertog shear zone in Greenland. Third, the differential stresses associated with deformation in these fault zones, as well as the strengths and limitations of this new technique, are discussed.

## 2. PALEOSTRESS SCALES

As a good, first-order approximation, the dislocation density, subgrain size, and grain size generated during plastic deformation depend only on the magnitude of the differential stress. Temperature has a minor influence on these three quantities through materials parameters such as the shear modulus. The dislocation density, subgrain size, and grain size can be thought of as depending upon temperature and strain rate, of course, because temperature,  $T$ , strain rate,  $\dot{\epsilon}$ , and the differential stress,  $\sigma_1 - \sigma_3$ , are coupled through a flow law

$$\dot{\epsilon} = f(\sigma_1 - \sigma_3) \exp[-(Q + PV)/RT] \quad (1)$$

where  $f(\sigma_1 - \sigma_3)$  is a function of the applied stress,  $Q$  is the activation energy for creep,  $V$  is the activation volume for creep,  $P$  is the hydrostatic pressure, and  $R$  is the gas constant. However, physically it is the differential stress or force to which dislocations respond; temperature/strain rate governs the kinetics of their response.

### 2.1 Dislocation Density - Differential Stress

The theoretical justifications for the empirical relations between applied stress and dislocation density, subgrain size, and grain size are incomplete. Yet, the qualitative arguments involved illustrate the basic physical considerations that are important in such theories.

The reasoning most frequently used to explain the stress-dislocation density relation has been clearly summarized by Nicolas and Poirier (1976, pp. 127-128). Each dislocation elastically strains the crystalline lattice and, as a result, has a stress field associated with it. Neighboring dislocations interact with (exert forces on) one another through their stress fields. The stress at any point in the crystal,  $\sigma_{\text{local}}$ , is

$$\sigma_{\text{local}} = (\sigma_1 - \sigma_3) - \sigma_{\text{int}} \quad (2)$$

where  $\sigma_1 - \sigma_3$  is the applied or differential stress and  $\sigma_{\text{int}}$  is the internal stress field due to all of the dislocations in the crystal. When the local stress falls below the critical stress required to operate dislocation sources (such as Frank-Reed sources), dislocation multiplication ceases and a steady-state dislocation density is established. If the density of free dislocations decreases due to dislocation-dislocation annihilation or dislocation climb into subboundaries, the internal stress decreases and the local stress increases permitting dislocation sources to operate again. This model assumes that the dislocation multiplication rate is fast compared to the rate at which dislocations are annihilated or absorbed into low angle boundaries.

The dislocation density can be determined as a function of the applied (differential) stress by assuming that the applied stress is proportional to the internal stress,

$$\sigma_1 - \sigma_3 \propto \sigma_{\text{int}} \quad (3)$$

In turn, from elasticity theory, the internal stress felt by a nearest-neighbor dislocation due to a given dislocation is proportional to the inverse of the distance,  $r$ , from that dislocation

$$\sigma_{\text{int}} \propto \frac{\mu b}{r} \quad (4)$$

where  $\mu$  is the shear modulus and  $b$  is the Burgers vector (the displacement vector associated with the dislocation's motion).

On geometrical grounds, the dislocation density,  $\rho$ , is simply related to the spacing between dislocations by the equation

$$\rho \approx \frac{1}{r^2} \quad (5)$$

Combining Eqs. (3), (4), and (5) leads to

$$\rho = \left( \frac{\sigma_{\text{app}}}{\alpha \mu b} \right)^2 \quad (6)$$

where  $\alpha$  is a materials constant of magnitude near one.

Others models/theories have been presented which also argue for a one-to-one correspondence between dislocation density and applied stress under conditions of plastic deformation. For the present discussion, the correctness

of one model versus another is unimportant. The important point is that dislocations interact via their elastic stress fields. Thus, for example, their density cannot increase indefinitely, and it is reasonable that a stress-determined, steady-state density is obtained. Dislocation density-applied stress data for a large number of materials (well in excess of 50 (see Takeuchi and Argon, 1976)) clearly demonstrate that the "steady-state" dislocation density increases as the applied stress increases, although the increase may be less rapid than the square of the applied stress (Goetze, 1978).

Dislocation density versus applied stress data are plotted in Fig. 1 for experimentally deformed olivine and quartz grains. A least squares fit of these data to Eq. 6 yields  $\alpha = 3$ . Durham et al. (1977) have fit a similar collection of data for olivine to the equation

$$\rho \propto (\sigma_1 - \sigma_3)^m \quad (7)$$

and obtain  $m = 1.6$ . The data presented in Fig. 1, including the recent results of Zeuch and Green (1978), extend over four orders of magnitude in dislocation density and are in good agreement with the  $m = 1.6$  value. The stress-dislocation density data for olivine in Fig. 1 cover a temperature range of 600°C, a strain rate range of 4 orders of magnitude, hydrostatic pressures between 1 and 15,000 bars, and different water contents. Clearly, the dislocation density is primarily determined by the differential stress.

While the data may deviate from the anticipated  $\rho \propto (\sigma_1 - \sigma_3)^2$  behavior, the empirically derived dislocation density-differential stress relation, Fig. 1, provides a sound basis for estimating paleostresses.

## 2.2 Dynamically Recrystallized Grain Size - Differential Stress

On the one hand, it might intuitively seem reasonable that the grain size should continually decrease as the strain in a sample is increased. Certainly, this situation is observed when deformation takes place by fracture/brittle mechanisms. A grain size reduction during plastic deformation is also common, although numerous examples of grain growth during plastic deformation are common (see, for example, Kamb, 1972). On the other hand, under static conditions at high temperatures (typically  $T > 0.5T_m$  for laboratory time scales) grain growth can be rapid in polycrystalline aggregates. Such grain growth enables the grain to reduce its total free energy by reducing its total grain boundary surface area and, thus, the energy associated with this surface area.

During high-temperature plastic deformation, grain boundaries migrate absorbing the free dislocations that they encounter. This situation is sketched in Fig. 2 (after Bailey and Hirsch, 1962). The grain boundary migrates upward into a region of high dislocation density. As a result, the dislocation density is locally decreased, as is the elastic strain energy due to the dislocations. With further deformation, the serrations or bulges along the grain boundary pinch off to form new grains. Because dislocations are continually generated, a steady-state condition is possible in which the increase in free energy per unit volume due to the increased surface area,  $E_Y$ , is balanced by the reduction in free energy per unit volume due to the decrease in dislocation density,  $E_P$ ,

$$E_Y \approx E_P \quad (8)$$

The grain boundary free energy per unit volume for a grain of diameter  $D$  is

$$E_Y \approx 3\gamma/D \quad (9)$$

where  $\gamma$  is the energy of the grain boundary. The free energy per unit volume for a density of dislocations  $\rho$  is (Friedel, 1964)

$$E_\rho = \rho\mu b^2 \quad (10)$$

The steady state grain size will be approximately

$$D \approx \frac{3\gamma}{\rho\mu b^2} \quad (11)$$

Using the empirical relation  $\rho \propto (\sigma_1 - \sigma_3)^{1.6}$  gives

$$D \propto (\sigma_1 - \sigma_3)^{-1.6} \quad (12)$$

As with the dislocation density, this analysis predicts a grain size sensitive to differential stress and not to temperature and strain rate.

Examples of migrating grain boundaries are common in naturally deformed quartzites. An optical micrograph of a section of the basal quartzite from the Ikertoq shear zone in Greenland is presented in Fig. 3. The quartz-quartz grain boundaries are highly serrated due to extensive grain boundary migration. A new generation of small grains is replacing the old, relict grains by dynamic recrystallization along the grain boundaries. As will be seen below in the discussion of the Moine thrust zone, specimens can be found in all proportions of new and old grains. When a quartz grain is surrounded by other phases, recrystallization often occurs within the quartz grain along low-angle subgrain boundaries, and not along the two-phase boundary. An example of this phenomenon in the gneiss from the Ikertoq shear zone is shown in Fig. 4.

In quartz, and possibly olivine, the grain boundary mobility is greatly increased by trace amounts of water (Hobbs, 1968). Thus, the percentage of a quartz sample that is recrystallized at a given differential stress for a certain strain should depend critically upon available water. (However, the grain size-stress relation appears to be unaffected by the OH-content).

Dynamically recrystallized grain size versus differential stress data are available for a number of materials (for a summary, see Twiss, 1977, and Bromley and Sellars, 1973). The data for most materials fit the relation

$$D \propto (\sigma_1 - \sigma_3)^{-n} \quad (13)$$

where  $1.2 \leq n \leq 1.7$ . For wet quartzite, Mercier et al (1977) find

$$D = 6.6 (\sigma_1 - \sigma_3)^{-1.4} \quad (14)$$

where  $D$  is in  $\mu\text{m}$  and  $(\sigma_1 - \sigma_3)$  is in kbar. For olivine in wet and dry dunites, they report  $n = 1.23$ , while Ross et al (1978) found  $n = 1.27$  and Post's data (1977) yield  $n = 1.49$ . Kohlstedt et al (1976) arrived at a similar relation between

stress and grain size for naturally deformed olivine-bearing rocks

$$D = 9(\sigma_1 - \sigma_3)^{-1.6} \quad (15)$$

based on differential stress levels determined from dislocation densities; in Eq. 15 the grain size is in microns and the stress is kilobars. The stress-grain size data of Kohlstedt et al (1976), Mercier et al (1977), Ross et al (1978) and Zeuch and Green (1978) are combined in Fig. 5. The agreement of the differential stress versus grain size data for the three studies is very good, leaving little doubt that the dynamically recrystallized grain size is, to a good first approximation, a function only of the applied stress. Temperature and water content are important only in controlling the kinetics of the recrystallization process and not in determining the steady-state grain size.

Similar arguments to those used to rationalize a steady state, stress-determined grain size can be employed to argue for a stress-determined spacing between low-angle boundaries (subgrain size). Certainly the most convincing argument is that for a wide range of materials, the subgrain size (low-angle boundary spacing) is observed to decrease with increasing stress (Takeuchi and Argon, 1976). Inverse relationships between stress and subgrain size,  $d$ , for olivine have been reported for olivine. Durham et al (1977) found

$$d \propto (\sigma_1 - \sigma_3)^{-1} \quad (16)$$

and Ross et al. (1978) report

$$d \propto (\sigma_1 - \sigma_3)^{-1.61} \quad (17)$$

The former is in good agreement with the relation commonly reported in the materials science literature (Takeuchi and Argon, 1976). Twiss (1977, Fig. 1) presents a summary of subgrain size - differential stress data for a number of materials on a non-dimensionalized plot of  $\log(\sigma_1 - \sigma_3/\mu)$  versus  $\log(d/b)$ .

### 3. APPLICATIONS TO FAULT ZONES

#### 3.1 Moine Thrust Zone, Scotland

Weathers et al. (1979) have recently reported a paleostress analysis of the deformation-induced microstructures of quartz-bearing rocks from the Moine thrust zone, Scotland. Their observations on the basal quartzite unit at the Stack of Glencoul briefly are summarized here. The microstructures at this locality provide an excellent example of the development of deformation-induced (dynamic) recrystallization.

At the Stack of Glencoul, the Moine thrust has Moine Schist emplaced over the basal quartzite (Fig. 6, location B). Development of the mylonites along the Moine thrust occurred during the Caledonian orogeny (see, e.g., Peach and Horne, 1930; Johnson, 1965). The first episode of Caledonian deformation and metamorphism is generally assigned to the interval 480 to 510 m.y.B.P. Subsequent, brittle deformation occurred on the Moine thrust in Late Silurian/Early Devonian time. The mylonites in the Moine thrust zone, which have been thoroughly described by Christie (1960, 1963), were chosen for paleostress analysis because the plastic deformation likely occurred during a single orogenic

episode, in Early Ordovician time, and under greenschist conditions. Thus, at the time the regional stress decayed, the temperature may have been low enough that the deformation-induced microstructures underwent negligible static recovery.

At the Stack of Glencoul, samples of the basal quartzite were collected along a path approximately normal to the thrust plane. The maximum possible sampling distance was 110 m from the quartzite-schist contact; the minimum distance was within a few centimeters of the contact.

### 3.1.1 Optical Microscopy

The basal quartzite 110 m from the contact between the quartzite and the overlying Moine Schist is an equigranular, white quartzite with a minor amount of fine-grained mica, probably sericite. The quartz grains have axial ratios of 1:1 to 2:1 (Fig. 7A). The average grain size is 0.5 to 1.0 mm; extinction in relict grains is undulatory. A generation of new grains, formed by recrystallization along grain boundaries of relict quartz grains, is present at less than 5% by volume. These aspects are illustrated in Figure 7A.

At 50 m from the fault, the percentage of recrystallized material is markedly increased, although the axial ratios of relict quartz grains are increased only slightly (Fig. 7B). Approximately 25% of the quartzite is recrystallized, either along grain boundaries or subgrain boundaries of relict grains. The size of the new generation of quartz grains is approximately 10-20  $\mu\text{m}$ . The relict quartz grains, now clearly elongated due to plastic deformation, have axial ratios of approximately 3:1. The overall appearance of the quartzite 50 m from the thrust is one of large, slightly oval, relict quartz grains in a matrix of small, recrystallized quartz grains. The relict quartz grains show extremely undulatory extinction.

At 5 to 10 m from the fault surface, the relict quartz grains are distinctly elongated (Fig. 7C). The average axial ratio of the relict grains is approximately 10:1. The percentage of recrystallization is only 30%. The quartzite is composed of elongated ribbons of relict quartz grains showing intensely undulatory extinction surrounded by masses of recrystallized grains approximately 10-20  $\mu\text{m}$  in size.

One meter from the fault surface, the quartzite is approximately 65% recrystallized (Fig. 7D). The few remaining relict quartz grains are extremely elongated with axial ratios of approximately 25:1.

At the contact of the quartzite with the Moine Schist, at the Stack of Glencoul, the quartzite is completely recrystallized (Fig. 7E); narrow regions of new grains **having nearly** the same extinction direction, interpreted as having originally been elongated relict quartz grains, suggest axial ratios of 80:1 to 90:1. The recrystallized grain size at the fault is 10-15 microns.

The progressive development of the deformation-induced microstructure in the basal quartzite unit at the Stack of Glencoul affects both the axial ratio of the relict grains and the percentage of recrystallized quartzite. Far from the fault, the mildly deformed (low strain) quartzite is characterized by undulatory extinction in the nearly equant relict grains and by a minor amount of a new generation of grains formed by dynamic recrystallization. In the

severely deformed quartzite near the thrust surface, the relict quartz grains are extremely elongated and almost entirely recrystallized. In marked contrast to the progressively changing axial ratios of relict quartz grains and percentage of recrystallization, the size of the new grains formed by recrystallization is independent of distance from the fault; it remains at approximately 15  $\mu\text{m}$ .

### 3.1.2 Electron Microscopy

Six transmission electron micrographs showing the typical dislocation structure observed in quartz grains from the Moine thrust are presented in Figure 8. No qualitative differences were detected in the dislocation structure from one locality to the next or from one rock type to the next.

There are several important features of the dislocation structure in the quartz grains. First, a high density of low-angle tilt and twist boundaries subdivide each grain. The average spacing between neighboring, low-angle boundaries is 2  $\mu\text{m}$ , approximately one-tenth the average size of the recrystallized grains. The dislocations in the subboundaries or cell walls are uniformly spaced. Second, the free dislocations (those dislocation segments lying between low-angle boundaries) are frequently curved and are usually not confined to a single plane. Third, the distribution of free dislocations is quite homogeneous. No dense, steelwool-like dislocation tangles, which are characteristic of the localized slip bands produced in many of the high-stress (low-temperature, high-strain rate) laboratory experiments (Ardell et al., 1973), were observed.

All of these features are suggestive of a low-stress (high-temperature, low-strain rate) deformation history. Dislocation recovery mechanisms, such as cross slip and climb, are evident from the well-organized low-angle boundaries, the numerous curved dislocations, and the homogeneity of the dislocation distribution.

In Figure 9, the dislocation density versus the distance from the fault surface is plotted for the basal quartzite at the Stack of Glencoul. A log scale was used on the distance axis to permit a more detailed view of any changes occurring near the contact. The density of free dislocations was measured in thirty samples from the Moine thrust zone. For each sample, an area of approximately 1000  $\mu\text{m}^2$  was recorded on 24 transmission electron micrographs. The error bars used in Figure 9 represent one standard deviation in the density. The densities were determined by simply counting the number of dislocations per micrograph; no attempt was made to measure the line length per unit volume. A large portion of the scatter in the data may be due to this technique.

The striking feature of Figure 9 is the near constancy of the dislocation density along a line normal to the fault. The average dislocation density in quartz grains from the overthrust schist at the Stack of Glencoul is approximately the same as that in the underlying quartzite,  $\sim 5 \times 10^8 \text{ cm}^{-2}$ .

### 3.2 Ikertoq Shear Zone, Western Greenland

There are three major shear zones, or transcurrent fault systems, in Precambrian rocks of western Greenland, at about 65°-67°N latitude, in the vicinity of Holsteinsborg. They are the Nordre Stromfjord, the Ikertoq-Sondre Stromfjord (hereafter, Ikertoq) and the Evighedsfjord. A fourth, the Vesterland, is at about 62°N latitude, south of Godthab. The zones, up to 40 km wide, are in urcaean gneisses; they are thought to have formed before 1600 m.y.B.P. The



shear zones have affected subsequent geologic evolution of the region, as zones of crustal weakness and movement, from Late Archean to Recent time (Watterson, 1975). The Nordre Stromfjord and Ikertoq are in the Nagssuguoqidian mobile belt which is bounded on the south, about mid-way up Sondre Stromfjord, by the "Archean block" (Bak et al., 1975). The region is being studied in detail by a joint British and Danish group of geologists, as a part of the International Geodynamics Project.

The Ikertoq shear zone extends from Holsteinsborg to east of the eastern end of Sondre Stromfjord. Rocks on either side of the Ikertoq zone are granodioritic to tonalitic gneisses that are complexly folded, migmatized, and in the granulite facies. They are probably equivalent to the Nuk gneisses of the Godthaab region, of approximately 2800 m.y. age. Bak et al. (1975), from an analysis of tectonite fabrics, suggest that the zone of plastic deformation within the Ikertoq shear zone, about 40 km wide, formed by right lateral displacement of approximately 200 km. The transcurrent shearing was followed by southward overthrusting within the Ikertoq.

The Kangerlussuaq dike swarm (Ramberg, 1948 ; Escher et al, 1976) cuts through the Sondre Stromfjord area. The dikes have been severely deformed as evidenced by the extensive boundinage. The dike rocks are metamorphosed to amphibolite facies.

### 3.2.1 Optical Microscopy

On a reconnaissance field trip to the Ikertoq shear zone near Sondre Stromfjord, a number of samples were collected of the gneiss and of the amphibolite. Characteristic microstructures in the gneiss and the amphibolite are shown in Figs. 10 and 11 respectively.

In the gneiss, Fig. 10, the microstructures of both the quartz and the feldspar grains indicate that gneiss has undergone extensive plastic deformation. The quartz grains running from left to right in Fig. 10A have been elongated to axial ratios of 2:1 to 5:1. They have been bent around more refractory neighboring feldspar grains. Numerous low angle boundaries subdivide the grains, and a new generation of recrystallized grains have replaced parts of the older grains. The average size of the new grains is in the range 25-50  $\mu\text{m}$ . The new grains are frequently elongated with an axial ratio of 2:1. A clearer picture of the low-angle boundary structure in quartz is seen in Fig. 10B. New grains in the process of being formed by migration of a low-angle ( $\sim 10^\circ$ ) boundary in quartz are present in Fig. 10C; the size of the new grains is 2 to 3 times the diameter of bulges along the subgrain boundary. No grain boundary migration is observed along the quartz-feldspar grain boundary. Figure 10D shows a deformed feldspar grain. The grain has not been noticeably elongated, although it is heavily twinned and shows undulatory extinction. The quartz grains from the dike, Fig. 11, appear to be somewhat less deformed (i.e. they appear to have undergone a smaller amount of strain) than the quartz grains in the gneiss. The relatively large quartz grain in Fig. 11A shows undulatory extinction, is subdivided by low-angle boundaries, and has an axial ratio of 2:1. No new feldspar grains formed by recrystallization are present. Smaller quartz grains, Fig. 11B and 11C, are generally less elongated and contain few low-angle boundaries than the larger grain in Fig. 11A. In marked contrast to the quartz grains, the amphibole grains show no signs, other than a planar fabric, of plastic deformation. For example, in Fig. 11C a  $120^\circ$  triple junction exists

within a few millimeters of a deformed quartz grain. The amphiboles appear to be fully recovered, except for an occasional low-angle boundary, Fig. 11D.

### 3.2.2 Electron Microscopy

A TEM survey of the dislocation structure in the quartz and amphibole grains reveals the following: Consistent with the optical observations, the quartz grains contain well-developed dislocation structures. Typical dislocation structures are present in Fig. 12. Three features stand out. First, this dislocation distribution is quite homogeneous. Second, subgrain structure is well developed. Third, the dislocations are often curved. All three of these points indicate that the dislocation structure developed under high-temperature, low-strain rate, low-stress conditions. Dislocation climb, a diffusion controlled process, and/or cross slip, a high-temperature process, are essential in developing these structures. The free dislocation density is in the range  $1-4 \times 10^8 \text{ cm}^{-2}$ . The subgrain size is between 5 and 10  $\mu\text{m}$ .

In sharp contrast to the dislocation structure in the quartz grains, the dislocation density in the amphibole is less than  $5 \times 10^6 \text{ cm}^{-2}$ . This density is so low that it is difficult to obtain a meaningful, statistical survey of the dislocation structure. At the TEM scale, compared to the quartz, the amphibole appears to be either fully recovered or undeformed.

## 4. DISCUSSION

### 4.1 Moine Thrust Zone

We emphasize the following results of this study.

(1) The dislocation density and the recrystallized grain size are independent of distance from the fault (Fig. 9). Also, the dislocation density is the same in the rock units on either side of the fault. Thus, the differential stress is independent of distance from the fault, at least within our sampling distance which was on the order of 100 meters.

The differential stress in the basal quartzite calculated from the dislocation density of  $5 \times 10^8 \text{ cm}^{-2}$  (using Fig. 1), the subgrain size of 2  $\mu\text{m}$  (using Fig. 1 in Twiss, 1977), and the recrystallized grain size of 15  $\mu\text{m}$  (using Eq. 14) is 1.3 kbar, 1 kbar, and 0.6 kbar, respectively. Therefore, we conclude that the microstructures in the basal quartzite were generated at a differential stress of  $1 \pm 0.5$  kbar. The uncertainty in this value will almost certainly decrease when more experimental data relating the differential stress to the resulting dislocation density, subgrain size, and grain size are available.

Twiss (1977) has pointed out that the size of recrystallized grains in quartz-rich mylonites from large thrust faults is commonly 10 to 40  $\mu\text{m}$ , corresponding to differential stresses from 0.25 to 0.75 kbar. For a shear zone in a granulite in the French Central Massif, Burg and Laurent (1978) found a differential stress between 0.5 and 1.5 kbar from dislocation density and subgrain size measurements. Briegel and Goetze (1978) obtained a differential stress of 2 kbar for the shear zone at the base of the Glarus overthrust; Switzerland, by analysis of the dislocation density in limestone. Thus, for the several shear zones sampled, the differential stresses consistently appear to be in the range 0.2 to 2 kbar. This range may be significantly narrowed when better calibrations

of the stress - microstructure scales are available.

(2) For a given fault zone, the differential stress determined from the dislocation density is generally a factor of two to three larger than that calculated from the recrystallized grain size. Two possible reasons for this discrepancy are proposed. First, the discrepancy could result from a long, low-stress episode of deformation followed by a short, high-stress pulse. In this situation, the recrystallized grain size, which changes more slowly with a stress change than does the dislocation density, still records the earlier, lower stress; the dislocation density, which equilibrates quite rapidly to a new stress level, measures the higher, more recent stress. Second (and we believe more likely), both the grain size - stress and the dislocation density - stress relations are based on very few data. The differential stresses estimated from either of the microstructural features could be in error by a factor of three or more.

(3) In the basal quartzite at the Stack of Glencoul, the axial ratio of the relict grains increases toward the fault (Fig. 7). This increase in the "intensity of deformation" or the "progressive deformation" implies that the strain, not the stress, increases toward the thrust. The natural logarithm of the axial ratio provides a rough estimate of the true strain undergone by the relict quartz grains.

Because the differential stress is independent of distance from the fault, the increase in strain toward the fault must correspond to an increase in strain rate. This increase in strain rate must, in turn, correspond to an increase in temperature, presumably due to strain or shear heating. An estimate of the temperature profile in the thrust zone can be obtained by assuming that the plastic deformation in the relict grains obeyed a flow law of the form

$$\dot{\epsilon} = f(\sigma)\exp(-Q/RT) \quad (4)$$

where  $\dot{\epsilon}$  is the strain rate,  $f(\sigma)$  is a function of the differential stress,  $Q$  is the activation energy for creep, and  $RT$  has the usual meaning. The temperature gradient calculated from the observed strain gradient (strain rate gradient) for  $Q = 30, 60, \text{ and } 90 \text{ kcal/mole}$  is approximately  $0.3, 0.45, \text{ and } 0.95^\circ\text{C/meter}$ .

(4) In the quartzite at the Stack of Glencoul, the percentage of recrystallized material increases toward the fault (Fig. 7). The amount of recrystallization correlates well with the plastic strain calculated from the axial ratio, i.e., the greater the strain the larger the percentage of recrystallized material. At the contact, 100% of the quartzite is recrystallized to an average grain size of  $15 \mu\text{m}$ .

This new, small grain size would have enhanced grain boundary deformation mechanisms, such as those involving grain boundary diffusion and sliding. It is likely that the grain-boundary contribution to the total strain rate would have exceeded the grain-matrix (e.g. dislocation) contribution. As a result, the strain would have been concentrated in the zone of fully recrystallized rock at the fault surface. The strain rate determined in regions containing both fine and coarse-grained material will be approximately the sum of the rates of the two types of mechanism.

(5) The deformation-induced microstructures are most readily analyzed in the quartzite. The schist was a fine-grained rock before the Moine thrust formed. Thus, the progressive elongation and recrystallization with increasing strain is not as striking in the schist as it was in the quartzite for which the pre-thrust grain size was large, ~1 mm.

(6) The presence of minerals other than quartz has several effects on the deformation of rocks. (a) The presence of muscovite inhibits the growth of recrystallized grains (Hobbs et al., 1976). In the gneiss, K-feldspar and plagioclase appear to have a similar effect. (b) These minerals constrain the deformation and elongation of the relict quartz, which apparently is the least refractory phase at the deformation conditions which existed during thrusting. (c) The grain boundaries between K-feldspar or plagioclase and quartz have a much lower mobility than those between two quartz grains. Thus, recrystallization occurred within quartz grains, generally along low-angle boundaries, rather than at the less mobile two-phase boundaries. (d) The undulatory extinction tends to be more intense in the quartz grains in the gneiss than in those in the quartzite. Recrystallization of quartz in the gneiss apparently required more strain than in the quartzite due to the numerous, immobile two-phase grain boundaries. For the gneiss and the schist, all of these effects obscure the progressive changes in microstructure which were observed in the quartzite. In addition, they complicate quantitative determinations of the differential stress from grain size measurements, because the grain size - stress scale was calibrated for quartzite. The dislocation density in the quartz grains, however, should depend only on the differential stress level, independent of the structure or composition of the neighboring grains.

(7) Several observations indicate that the deformation-induced microstructures are "frozen-in;" that is, little or no static annealing followed the main thrusting event. First, the small recrystallized grains would grow quickly under static annealing conditions. Second, the grain boundaries are often serrated as is typical of a severely deformed material, and 120° triple junctions characteristic of a recovered microstructure are rare. Third, the free dislocation density is large; experiments in our laboratory indicate that this density decreases rapidly during annealing. Fourth, the differential stresses estimated from the dislocation density, subgrain size, and grain size are in reasonably good agreement; the differences are probably due to calibrations of the various paleostress scales. Agreement amongst the three microstructural features is difficult to achieve unless the stress was roughly constant for a relatively large strain (>> 100%) because the recovery kinetics of the three features are drastically different.

#### 4.2 Ikertoq Shear Zone

The dislocation structures in the quartz grains from the gneiss in the Ikertoq shear zone are very similar to those in quartzites and gneisses from the Moine thrust zone. The dislocation distribution is homogeneous, dislocations are curved, and the low-angle tilt and twist boundaries are composed of uniformly spaced dislocations. All three features indicate a high-temperature, low-strain rate, low-stress deformation.

The dislocation density, subgrain size, and grain size correspond to differential stresses of 0.5 to 1.1 kbar, 0.2 to 0.4 kbar, and 0.2 to 0.4 kbar, respectively. Again, the differential stress based on the dislocation density

is a factor of 2 to 3 larger than that estimated from the grain size. More experimental data are required to better calibrate these paleostress scales.

### 4.3 General Comments

(1) What do we learn with certainty from these microstructural measurements?

Clearly, the application of these paleostress scales can provide estimates of the differential stresses during faulting, as well as other geologic deformation events. When the paleostress scales for quartz are better calibrated, stress determinations will be possible to within a factor of two or better. The dislocation density and grain size paleostress relations for olivine are already known to this accuracy.

(2) What are the limitations?

If the deformation event of interest is followed either by a static annealing or by another deformation, then the microstructural information of interest can be erased. In general, the last thermal-mechanical episode is recorded.

However, because the recovery rates for the grain size is much slower than that for the dislocation density, it is possible to record two deformation events or a deformation plus an annealing event in the microstructure. The dislocation density is always characteristic of the last significant episode of deformation or recovery; the grain size can retain information from a preceding episode. Goetze (1975) has convincingly demonstrated this point. Careful geologic field work is essential in determining which thermal-mechanical event imprinted the observed microstructures.

(3) What aspects of the paleostress relations require further research?

One major area requiring additional work is the experimental calibration of the paleostress scales for quartz over a wide range of test conditions. Similar measurements on other minerals (feldspars, amphiboles, etc.) would greatly increase the constraints on the thermal-mechanical history of a particular geologic deformation event. Several stages of the event could be assessed if the kinetics of recovery and deformation differ for the various minerals present.

Also, laboratory studies of the recovery kinetics in quartz, as well as other minerals, are needed. At present, it is difficult to estimate the times and temperatures required to alter a deformation-induced microstructure. In a similar manner, experiments designed to follow the development of steady-state microstructures are important. In the best of situations, it may prove possible to determine paleostress levels from partially recovered dislocation structures. For example, Goetze and Kohlstedt (1973) have demonstrated that during *isothermal* annealing of naturally deformed olivine the dislocations move into low-angle boundaries; the starting dislocation structure can be worked out by noting that the ratio of free dislocations to those in subboundaries prior to annealing was approximately 2:1.

Finally, combined field and laboratory studies are essential in order to test the range of settings for which this new technique can be applied.

## REFERENCES

- Ardell, A.J., Christie, J.M., and Tullis, J.A., Dislocation substructure in deformed quartz rocks, *Crystal Lattice Defects*, 4, 275, 1973.
- Bailey, J.E. and Hirsch, P.B., The recrystallization process in some polycrystalline metals, *Proc. Roy. Soc. A*, 267 11-30, 1962.
- Bak, J., Korstgard, J., and Sorenson, K., A major shear zone within the Nagssugtoqidian of western Greenland, *Tectonophysics*, 27 191-209, 1975.
- Briegel, U., and Goetze, C., Estimates of differential stress recorded in the dislocation structure of Lochseiten limestone (Switzerland), *Tectonophysics*; 48, 61, 1978.
- Bromley, R., and Sellars, C.M., High temperature deformation of copper and copper-aluminum alloys, in *The Microstructure and Design of Alloys, Proceedings of the Third International Conference on the Strength of Metals and Alloys*, 1, p. 380, 1973.
- Burg, J.P., and Laurent, P., Strain analysis of a shear zone in a granodiorite, *Tectonophysics*, 47, 15, 1978.
- Christie, J.M., Mylonitic rocks of the Moine Thrust zone in the Assynt region, north-west Scotland, *Geol. Soc. Edinburgh Trans.*, 18, 79, 1960.
- Christie, J.M., The Moine Thrust zone in the Assynt region, Northwest Scotland, *Univ. Calif. Publ. Geol. Sci.*, 40, 345, 1963.
- Durham, W.B., Goetze, C., and Blake, B., Plastic flow in oriented single crystals of olivine, Part 11. Observations and interpretations of the dislocation structures, *J. Geophys. Res.*, 82, 5755, 1977.
- Escher, A., Jack, S., and Watterson, J., Tectonics of the North Atlantic Proterzoic dike swarm, *Phil. Trans. R. Soc. Lond.* 280, 529-539, 1976.
- Friedel, J., *Dislocations*, Addison-Wesley, 491 pp, 1964.
- Goetze, C., Sheared Iherzolites: From the point of view of rock mechanics, *Geology*, 3, 172, 1975.
- Goetze, C., The mechanisms of creep in olivine, *Phil. Trans. R. Soc. Lond. A.*, 288, 99, 1978.
- Goetze, C., and Kohlstedt, D.L., Laboratory studies of dislocation climb and diffusion in olivine, *J. Geophys. Res.*, 78, 5961, 1973.
- Hobbs, B.E., Means, W.D., and Williams, P.F., *An Outline of Structural Geology*, John Wiley and Sons, Inc., New York, 1976.
- Hobbs, B.E., Recrystallization of single crystals of quartz, *Tectonophysics*, 6 353-401, 1968.

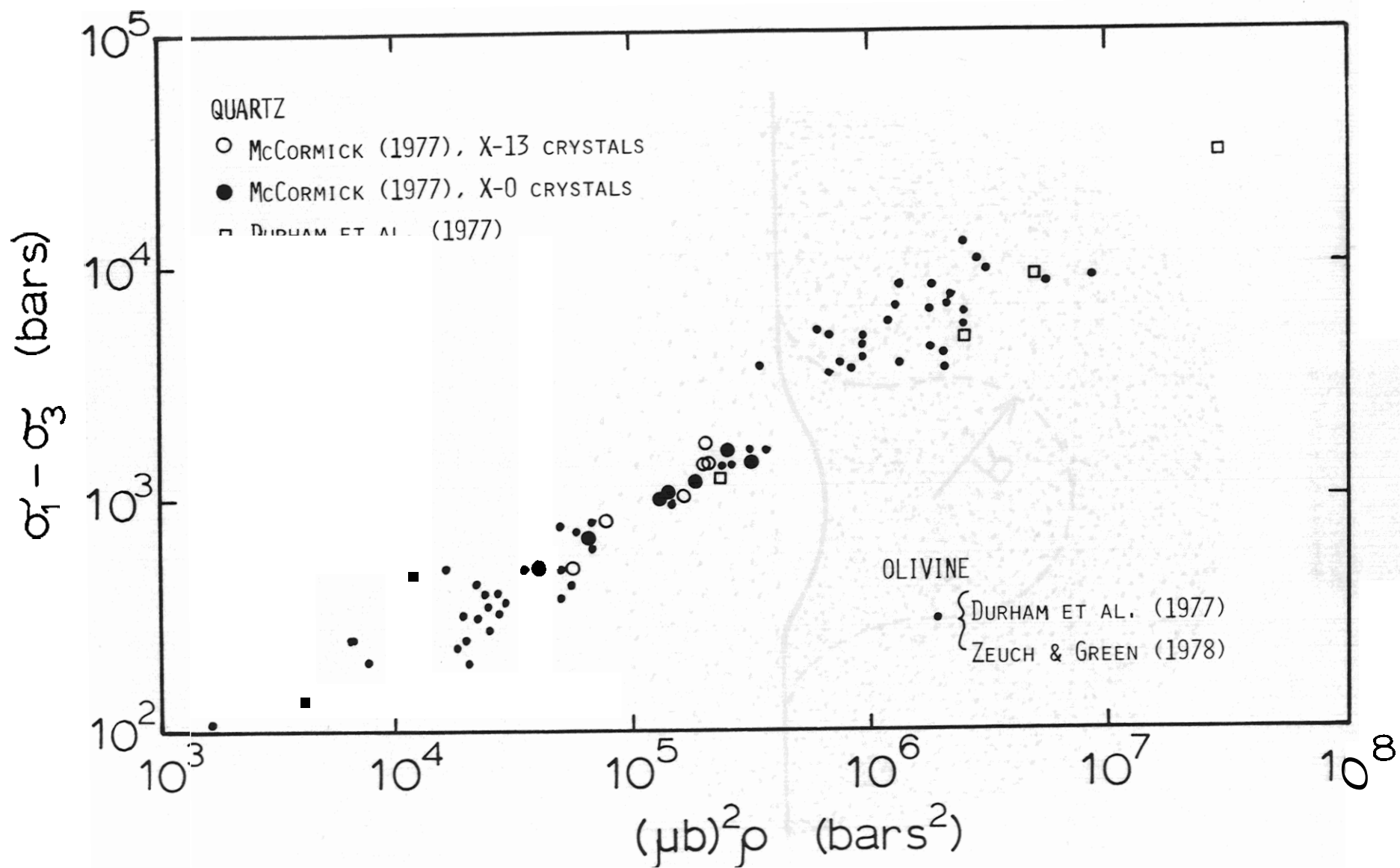
- Johnson, M.R.W., in The Geology of Scotland ed. Oliver and Boyd, London, 1965.
- Kamb, B. Experimental recrystallization of ice under stress, in Flow and Fracture of Rocks, eds. Heard, Borg, Carter, and Raleigh, AGU Monograph 16, pp. 211-241, 1972.
- Kohlstedt, D.L., Goetze, C., and Durham, W.B., Experimental deformation of single crystal olivine with application to flow in the mantle, in The Physics of Chemistry of Minerals and Rocks, edited by R.G.J. Strens, p. 35, John Wiley and Sons, Inc., New York, 1976b.
- McCormick, J.W., Transmission electron microscopy of experimentally deformed synthetic quartz, Ph.D. thesis, Univ. California, Los Angeles, 171 pp., 1977.
- Nicolas, A. and Poirier, J.P., Crystalline Plasticity and Solid State Flow in Metamorphic Rocks, John Wiley and Sons, 1976.
- Peach, B.N., and Horne, J., Chapters on the Geology of Scotland, Oxford University Press, London, 1930.
- Post, R.L., Jr., High-temperature creep of Mt. Burnet dunite, Tectonophysics, 42, 75, 1977.
- Ramberg, H., On the petrogenesis of the gneiss complexes between Sukkertoppen and Christianshab, west Greenland, Medd. Dansk Geol. Foren. 11, 312-327, 1948.
- Ross, J.V., Ave'Lallement, H.G., and Carter, N.L., Stress dependence of recrystallized grains and subgrain size in olivine, J. Geophys. Res., in press, 1978.
- Takeuchi, S., and Argon, A.S., Review: Steady state creep of single-phase crystalline matter of high temperatures, J. Material Sci., 11, 1542, 1976.
- Twiss, R.J., Theory and applicability of recrystallized grain size paleopiezometer, Pure Appl. Geophys., 115, 227, 1977.
- Watterson, J., Mechanisms for the persistence of tectonic lineaments, Nature 253 520-522, 1975.
- Weathers, Maura S., Cooper, Reid F., Kohlstedt, D.L., and Bird, J.M., Differential stresses determined from deformation-induced microstructures of the Moine thrust zone, accepted for publication, J. Geophys. Res., 1979.
- Zeuch, D.H. and Green, H.W., Experimental deformation of an "anhydrous" synthetic dunite, CNRS Intern. Colloq. on Deformation Mechanisms in Minerals and Rocks, 1-5 Oct. 1978.

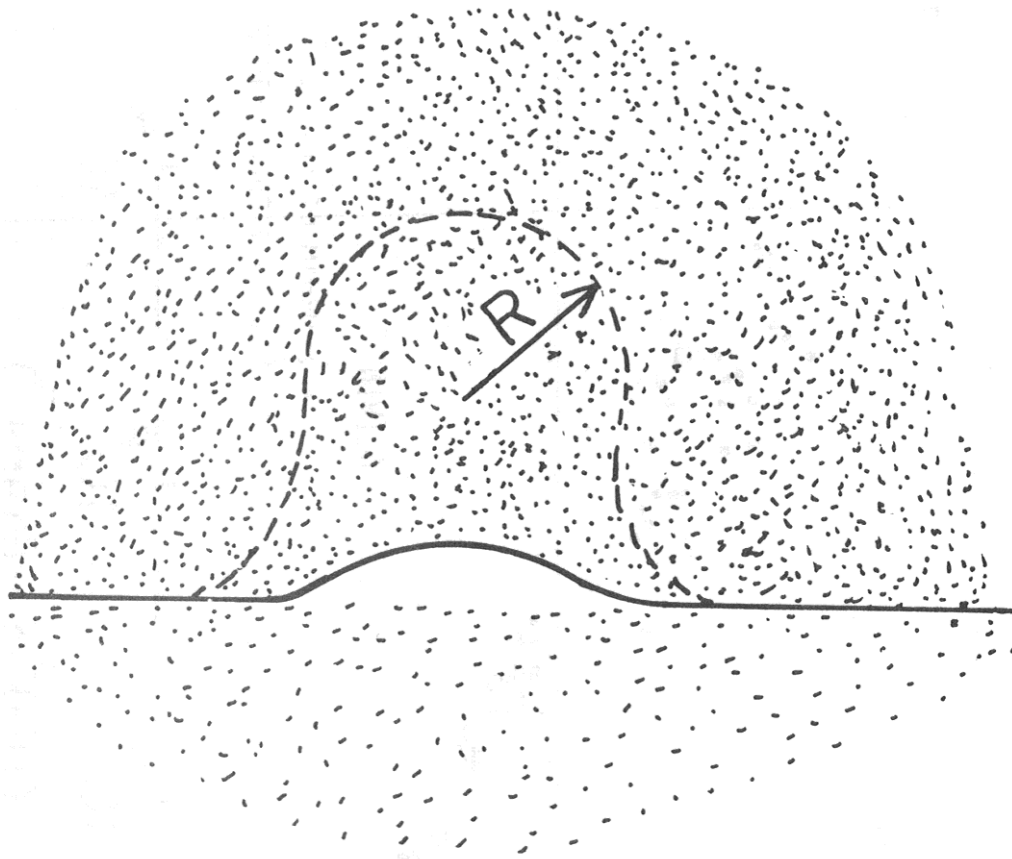
## FIGURE CAPTIONS

- Figure 1. Dislocation density as a function of applied, differential stress. Data for quartz and olivine are shown. To compare data for several materials, the dislocation density has been multiplied by the square of the shear modulus times the Burgers vector. Values of 0.65 & 0.44 Mbar and 5 Å & 5 Å were used for olivine and quartz, respectively. The increase in dislocation density with increasing differential stress is marked and systematic.
- Figure 2. Sketch of grain boundary migrating to consume high density of dislocations and lower elastic strain energy at the expense of increasing surface area. See also Fig. 3.
- Figure 3. Formation of recrystallized quartz grains. During deformation, relict quartz grains become elongated, developing serrated grain boundaries. With continued deformation, the serrations pinch off to form new quartz grains. See also Fig. 2.
- Figure 4. Deformation of quartz grain in gneiss from Ikertoq shear zone differs from that observed in the quartzite (see Fig. 3). Recrystallization of the quartz occurs along subgrain boundaries within quartz grains. Recrystallization did not occur along the relatively immobile quartz-feldspar grain boundaries.
- Figure 5. Grain size as a function of differential stress for olivine. The data of Mercier, Anderson, and Carter (1977) (M, A, & C) for wet and dry dunite are summarized by the dashed line. The data of Kohlstedt, Goetze, and Durham (1976) (K, G, & D) are shown and a best fit solid line is drawn. The open circles are data obtained from samples deformed in the earth with the stress determined from the dislocation density using Eq. 1 and Fig. 1. The solid circles are data taken from reported experimental results. The data of Ross, Ave'Lallement, and Carter (1978) (R, A, & C) are indicated by a dotted line, and that of Zeuch and Green (1978) (Z & G) by a dot-dash line.
- Figure 6. Location map of Moine thrust zone. The Stack of Glencoul is labeled B. Data from Geol. Surv. Great Britain (Scotland), Ordnance Survey of Great Britain, Sheet 5, (1948), and Christie (1963).
- Figure 7. Photomicrographs showing progressive deformation, basal quartzite at the Stack of Glencoul. Figure 7A, sample 120 m from fault; Figure 7B, 50 m from fault; Figure 7C, 10 m from fault; Figure 7D, 1 m from fault. Figure 7E, at the fault. Note progressive elongation of the relict quartz grains and increasing amount of recrystallization, approaching the fault.
- Figure 8. Transmission electron micrographs of typical dislocation structures in quartz grains, basal quartzite, Stack of Glencoul. Note numerous, low-angle boundaries in which dislocations are uniformly spaced, and the high density of curved free dislocations. The speckled background, which is most obvious in Figure 8E, is radiation damage (200 kV electron beam).



- Figure 9. Dislocation density in quartz grains, basal quartzite, versus log of distance from the Moine thrust fault at the Stack of Glencoul. Apparently, the dislocation density is independent of distance from the fault and averages  $4 \times 10^8 \text{ cm}^{-2}$ . Error bars equal one standard deviation.
- Figure 10. Photomicrographs showing deformation-induced microstructures in gneiss from the Ikertoq shear zone, near Sondre Stromfjord. Figure 10A, bent and partially recrystallized quartz. Figure 10B, low-angle tilt boundaries in quartz. Figure 10C, recrystallization along low-angle boundary in quartz. Figure 10D, deformed feldspar grain.
- Figure 11. Photomicrographs showing microstructures in dike rocks in Ikertoq shear zone, near Sondre Stromfjord. Figure 11A, undulatory extinction in quartz. Figure 11B, low-angle boundaries in quartz. Figure 11C, low-angle boundaries in quartz grain and  $120^\circ$  triple junction between amphibole grains. Figure 11D, tilt-boundary in amphibole grain.
- Figure 12. Transmission electron micrographs of quartz grains from gneiss in Ikertoq shear zone. Note the curved dislocations and well-developed low-angle boundaries.

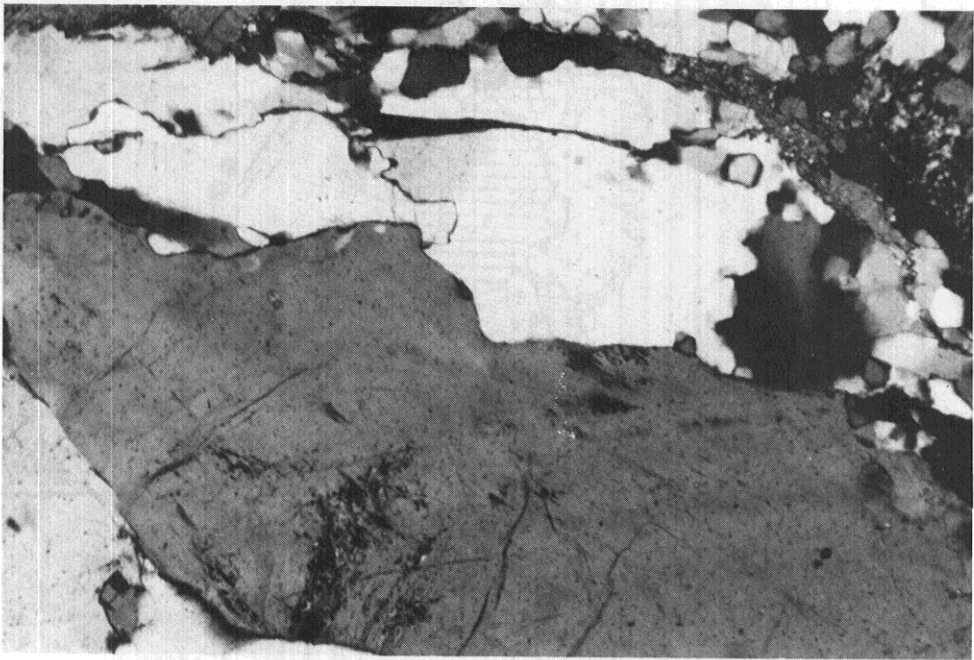






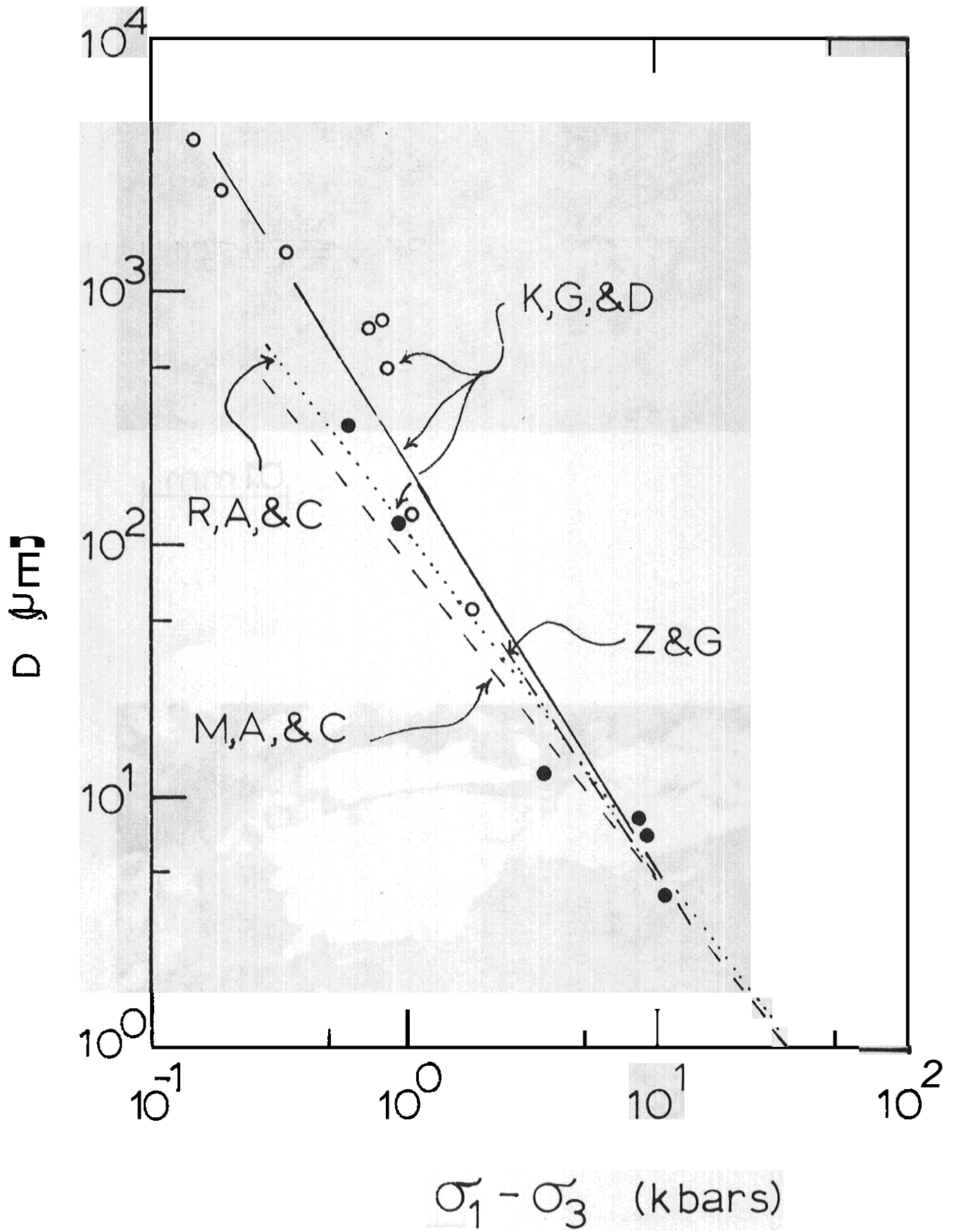
0.1 mm

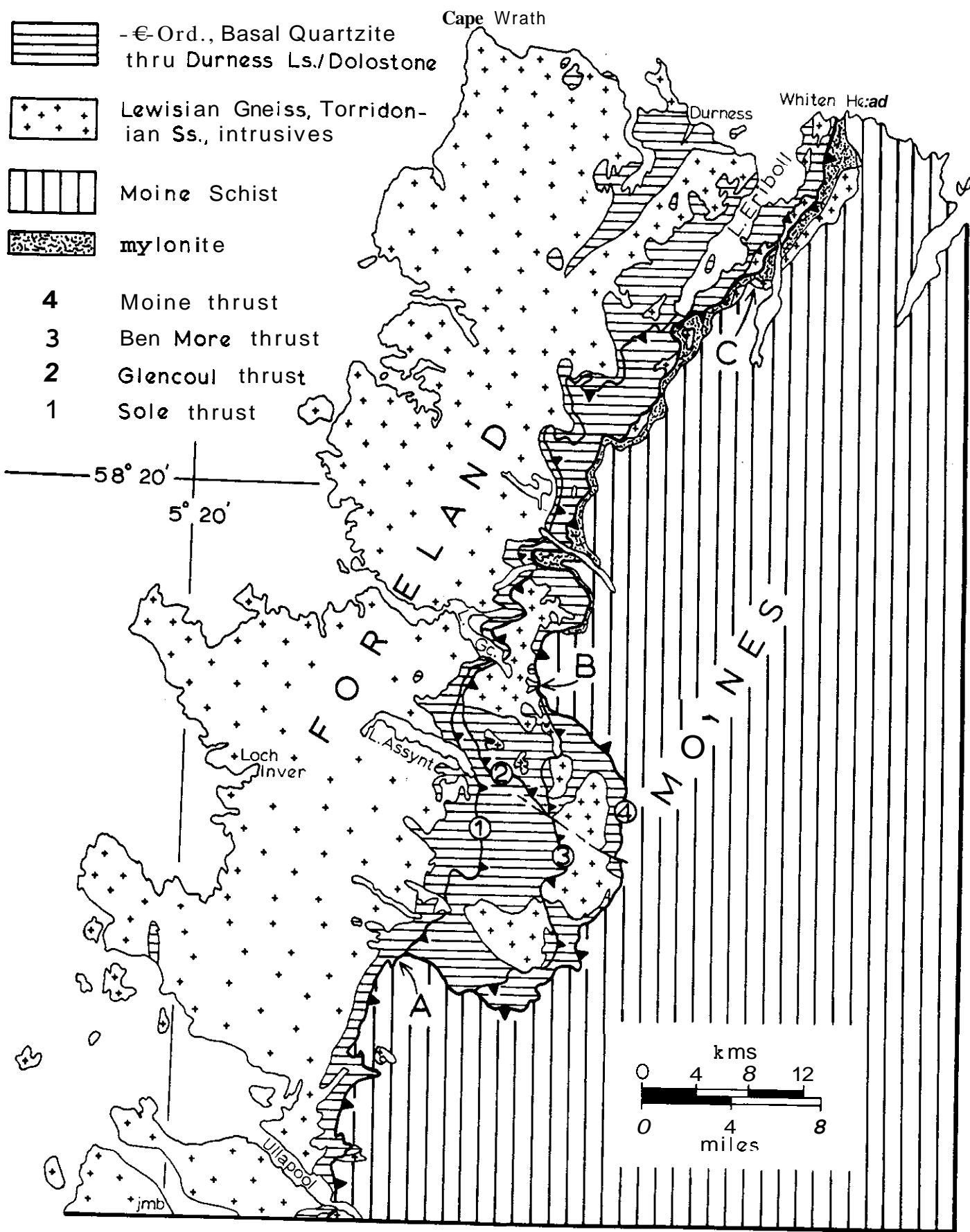
3

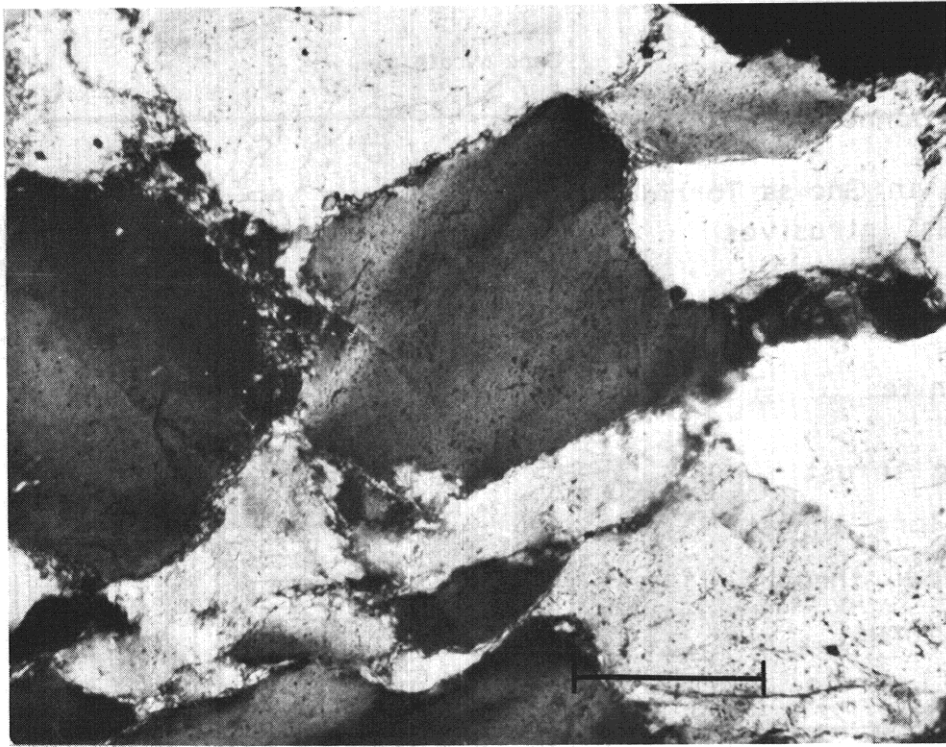


0.5 mm

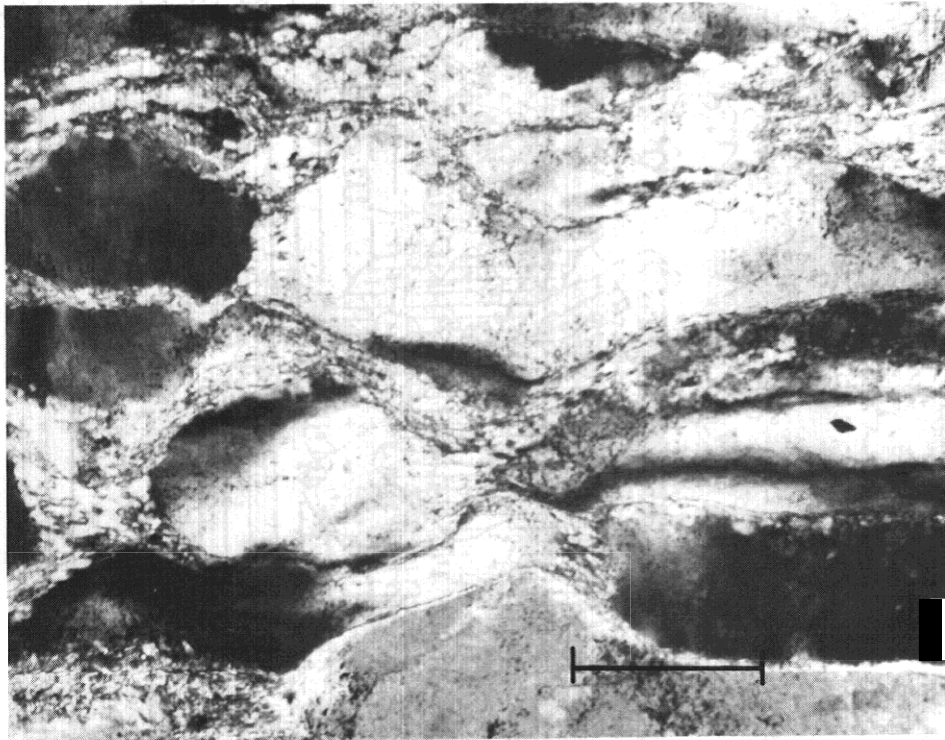
4



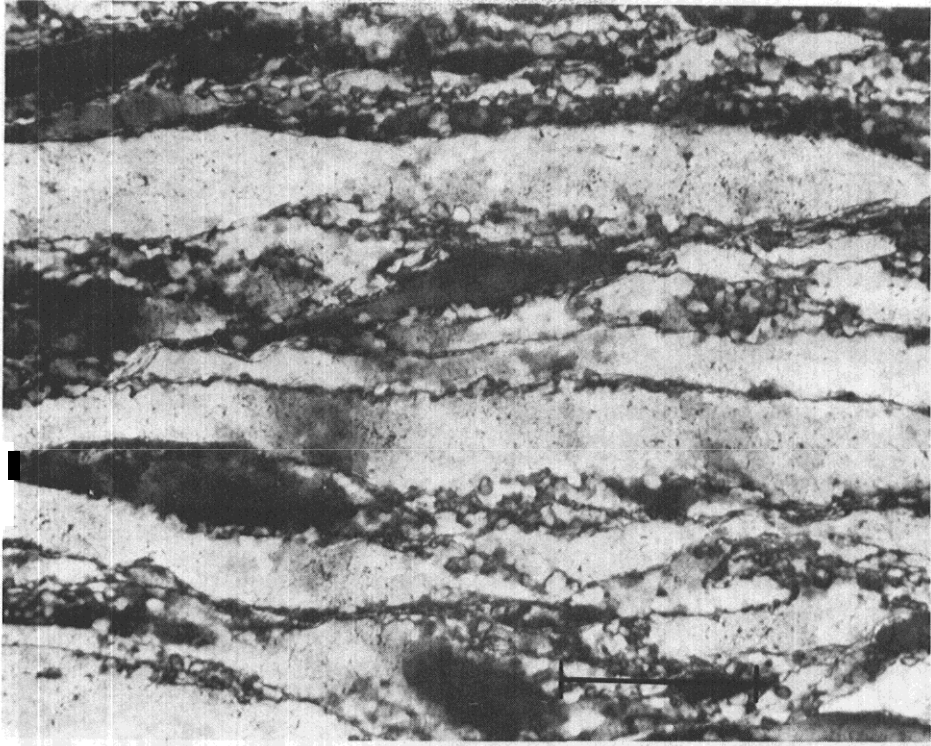




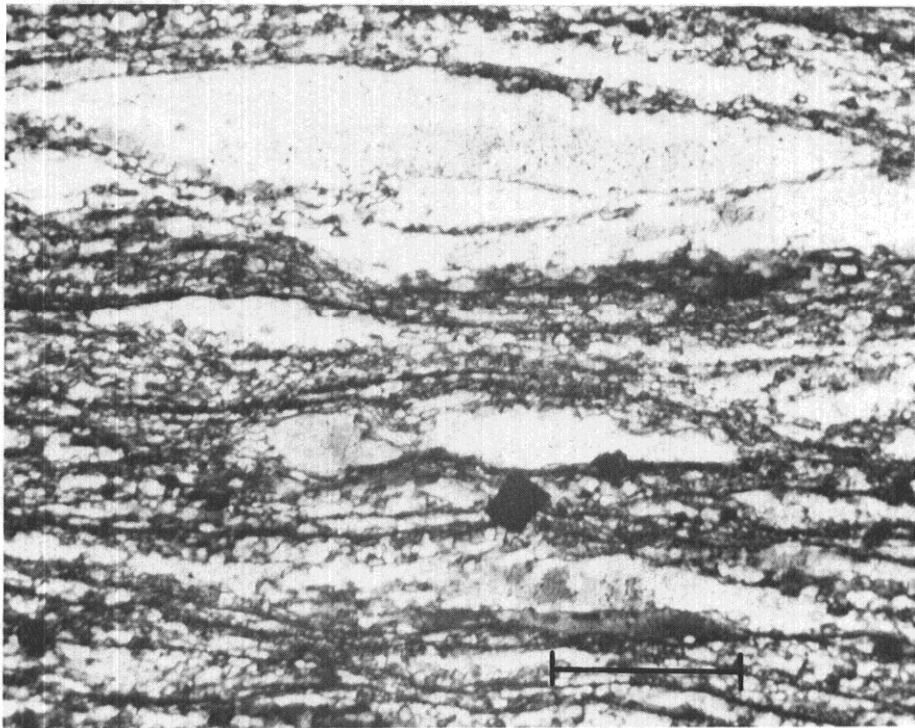
A



B

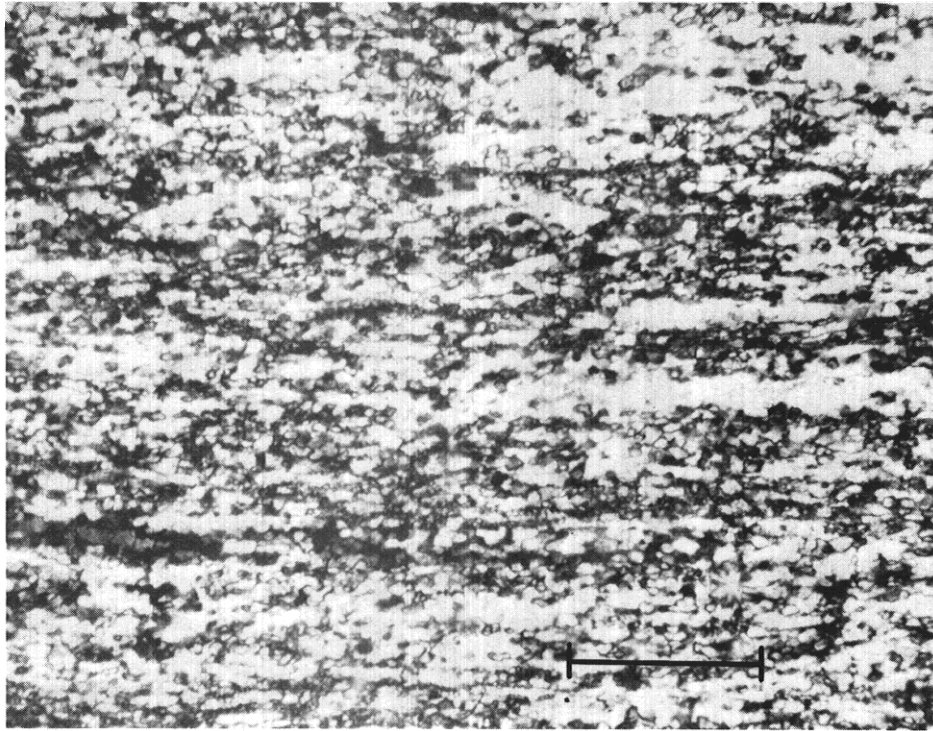


C



D



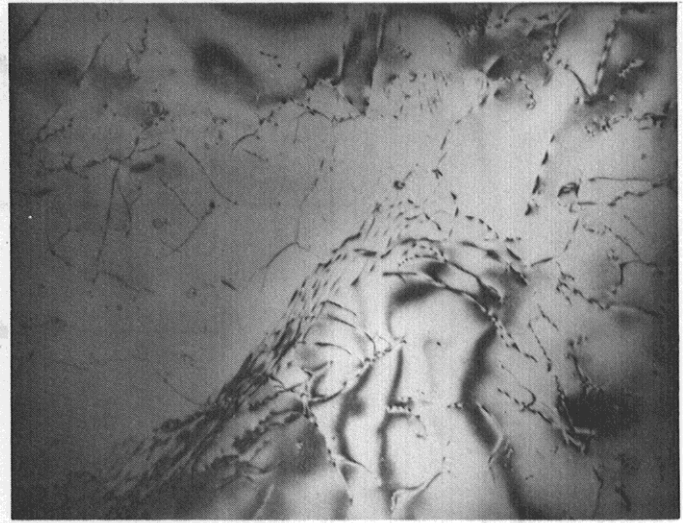
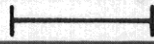


E

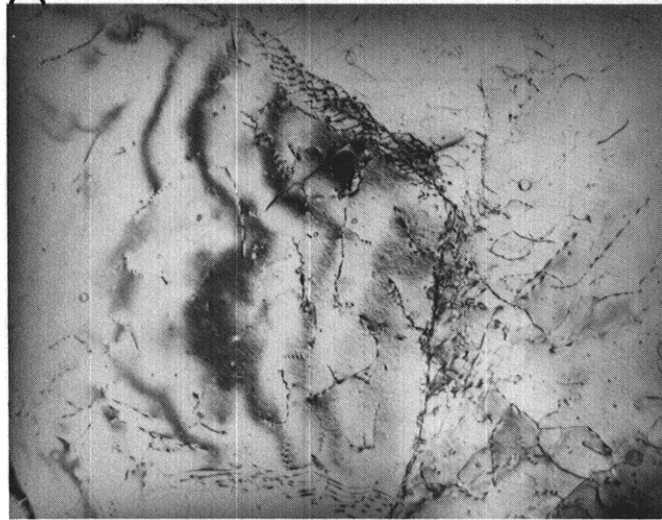
0.2mm



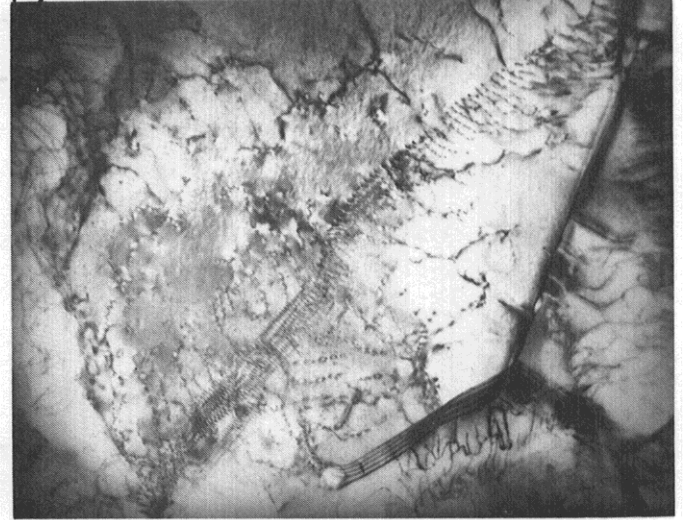
A



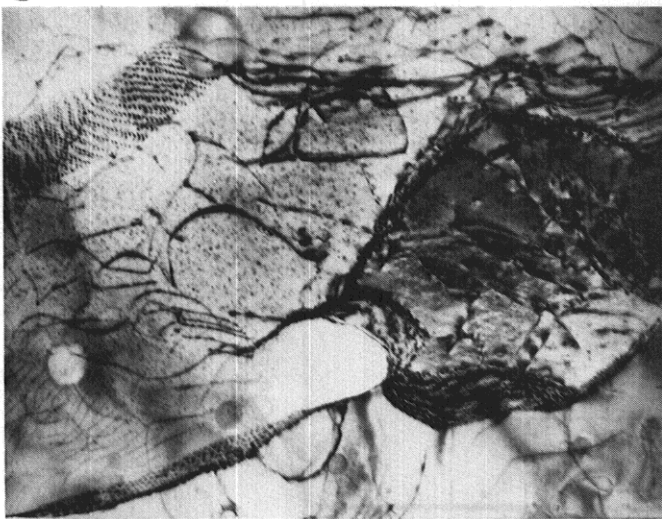
B



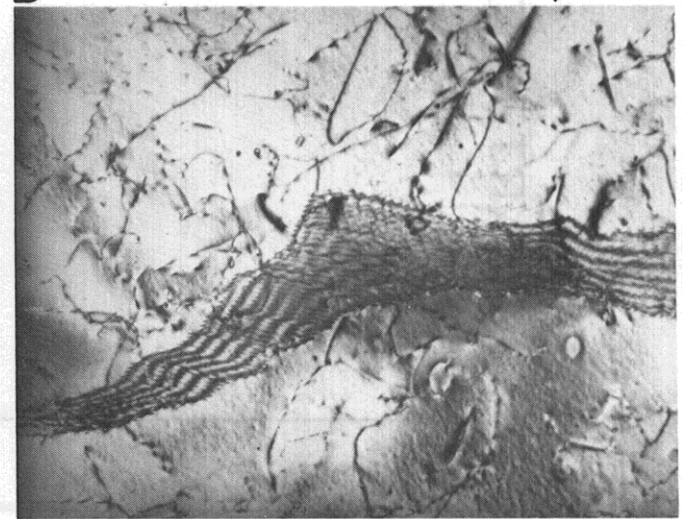
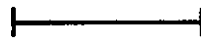
C



D



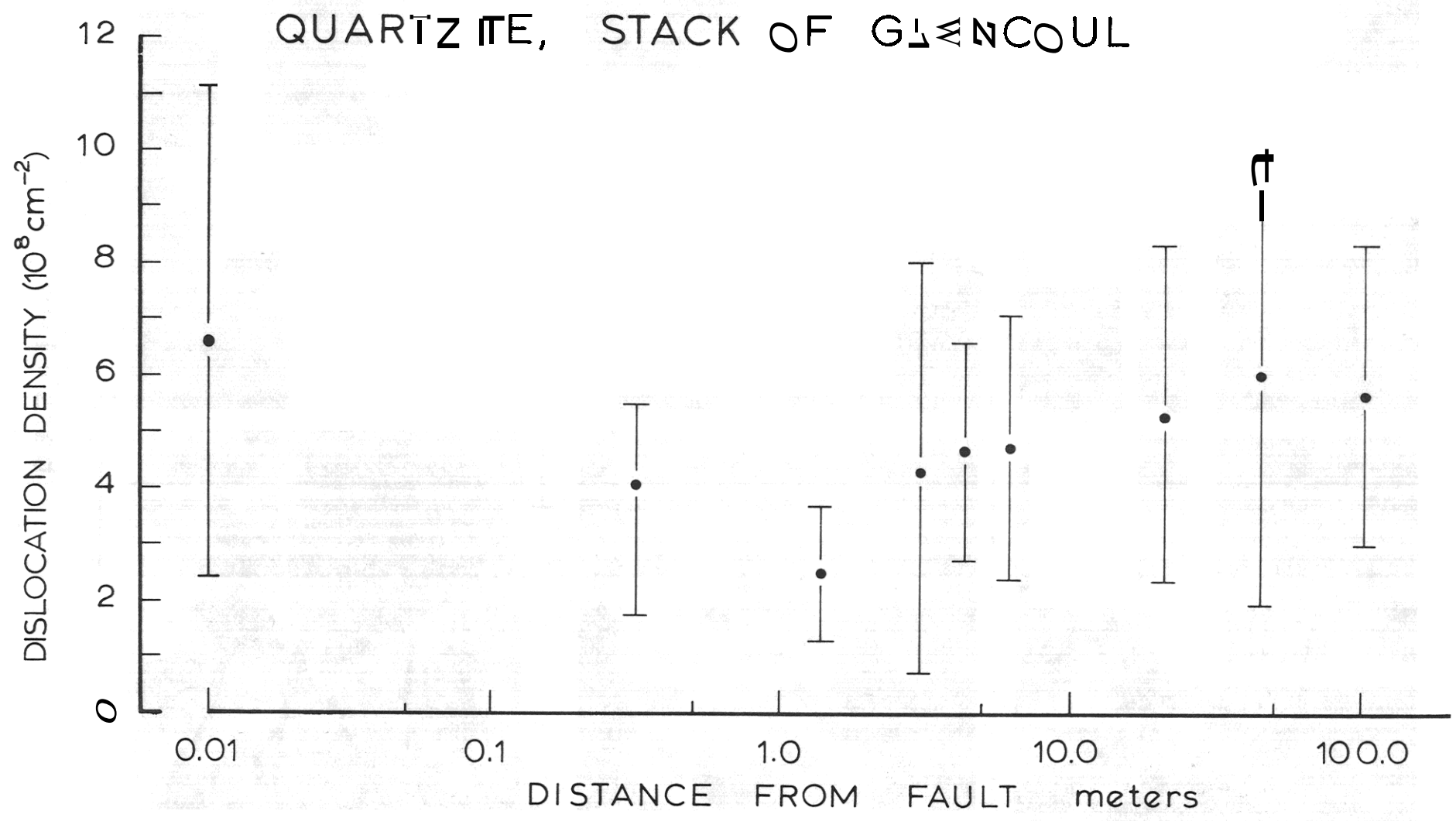
E

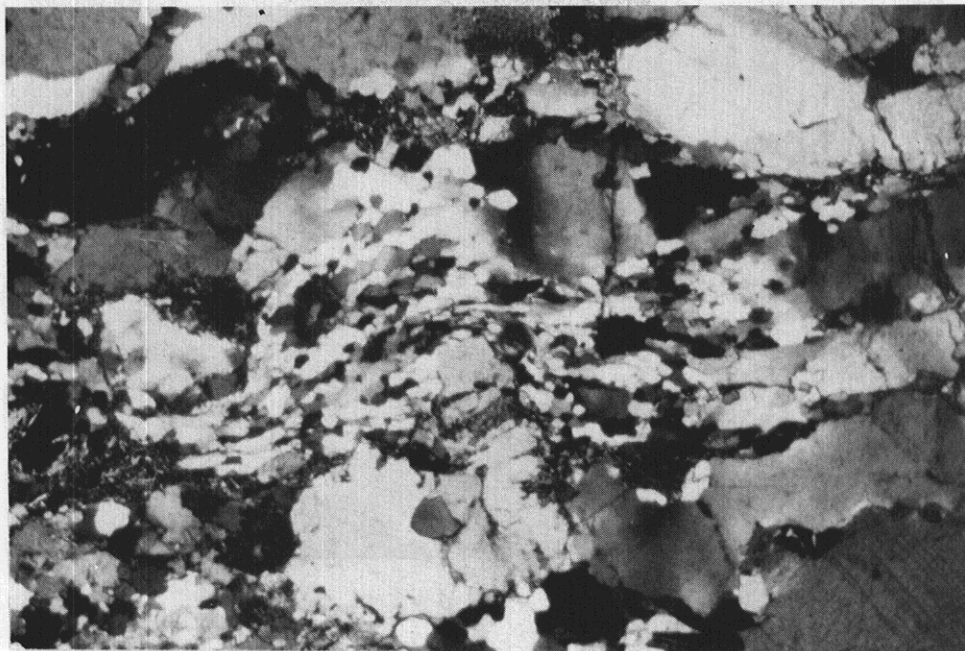


F

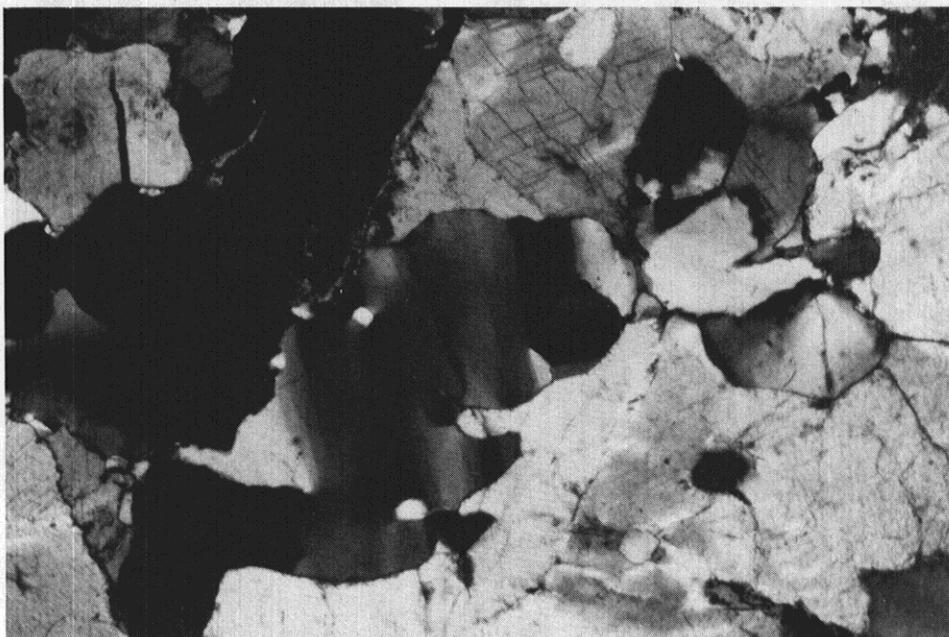
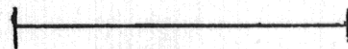


bars = 1  $\mu$ m

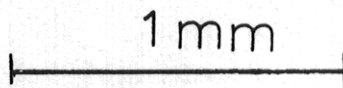


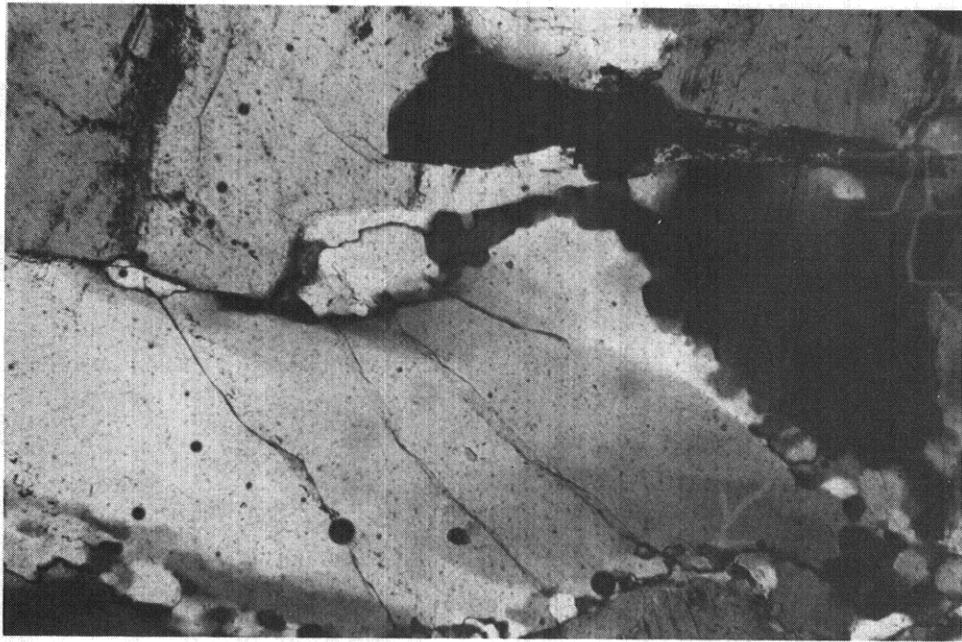


A

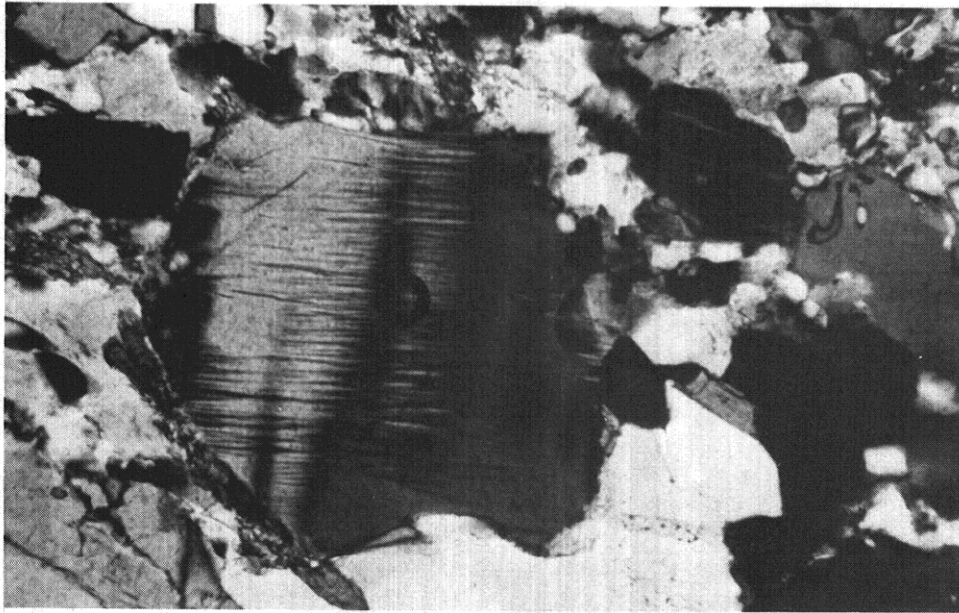


B

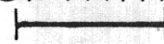


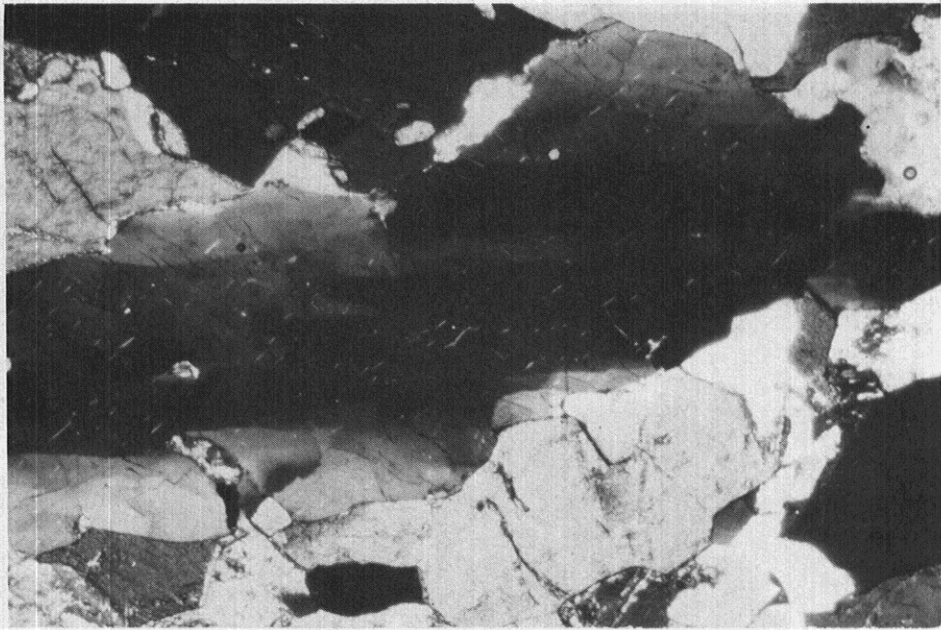


C

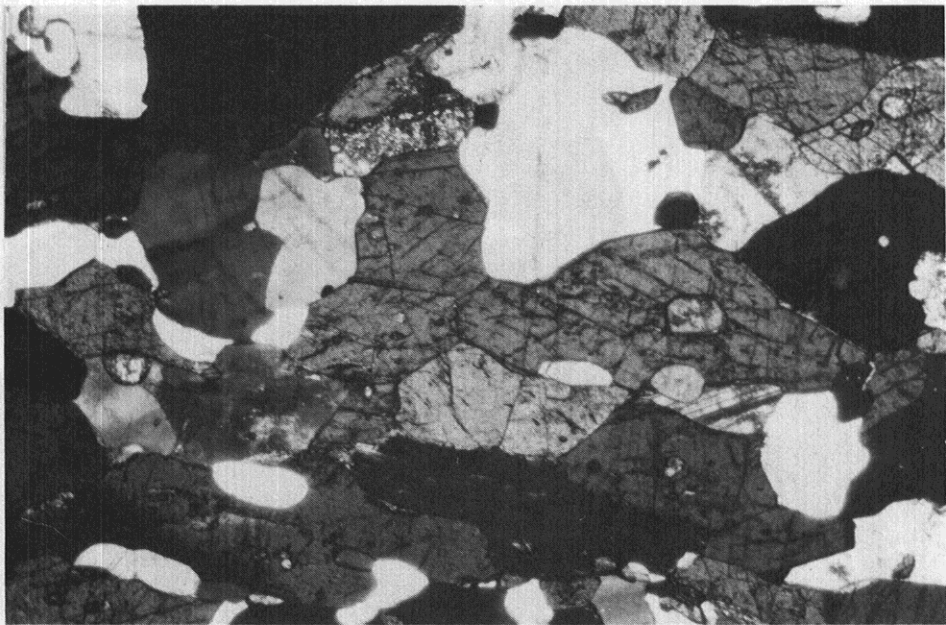


D

0.1 mm  


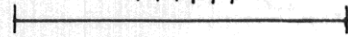


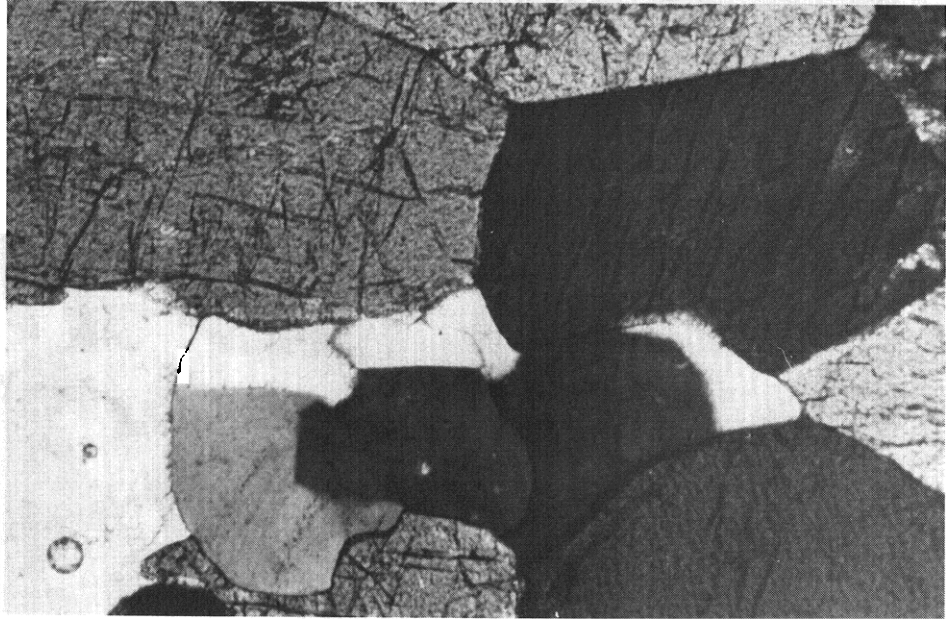
A



B

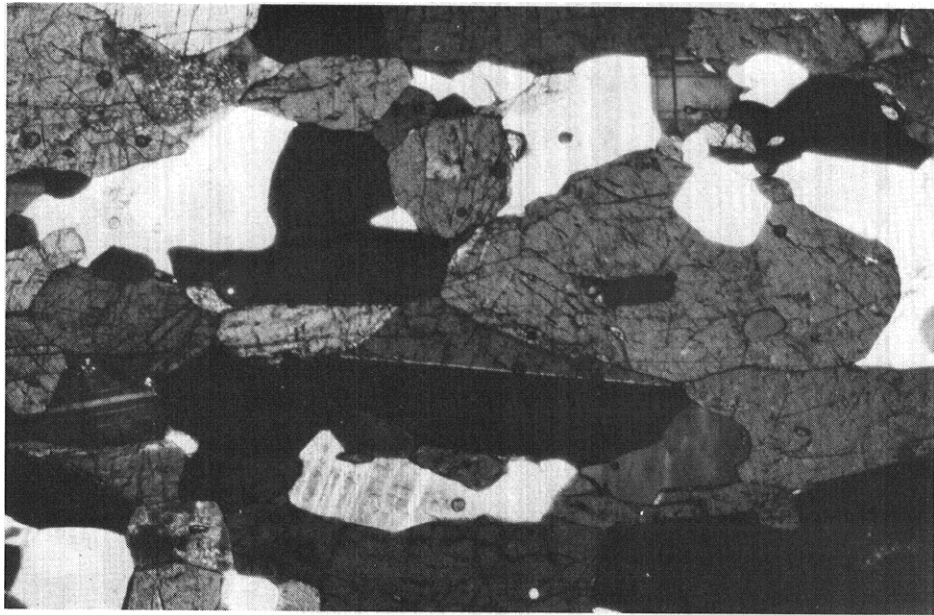
1 mm





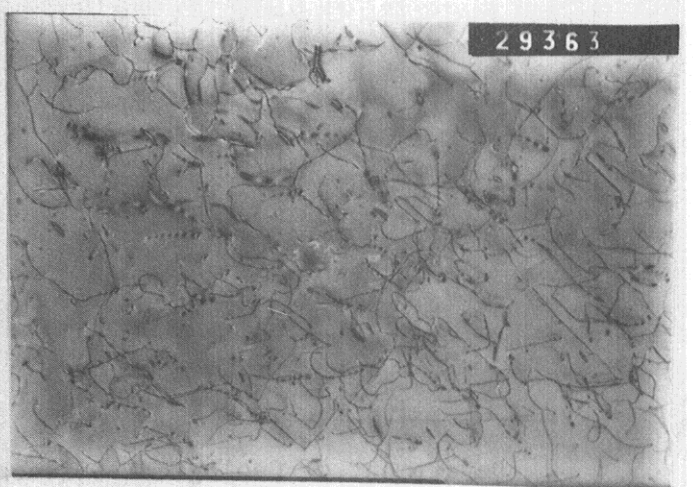
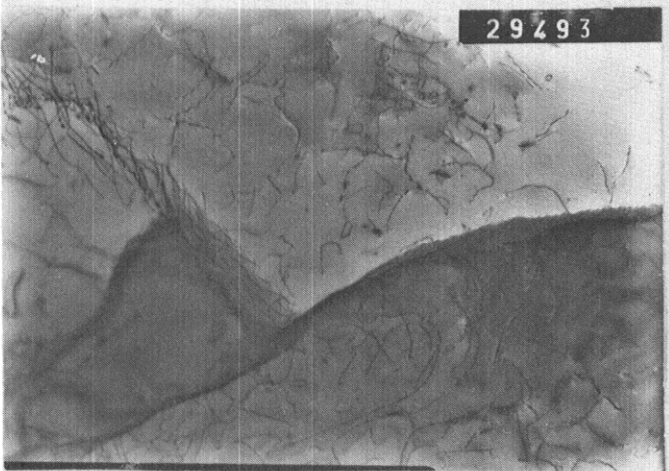
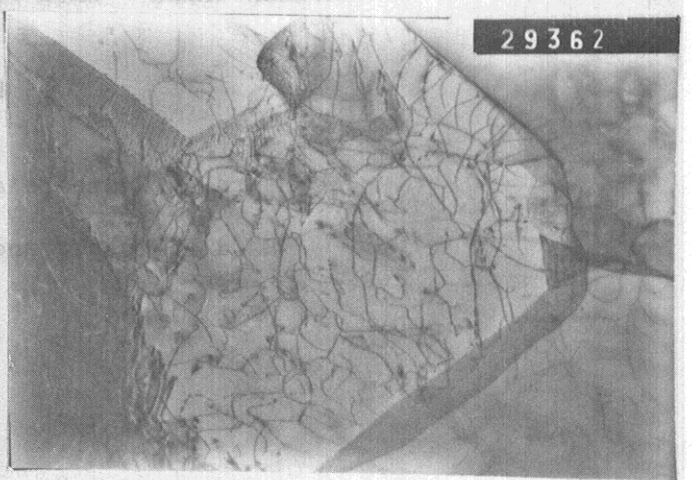
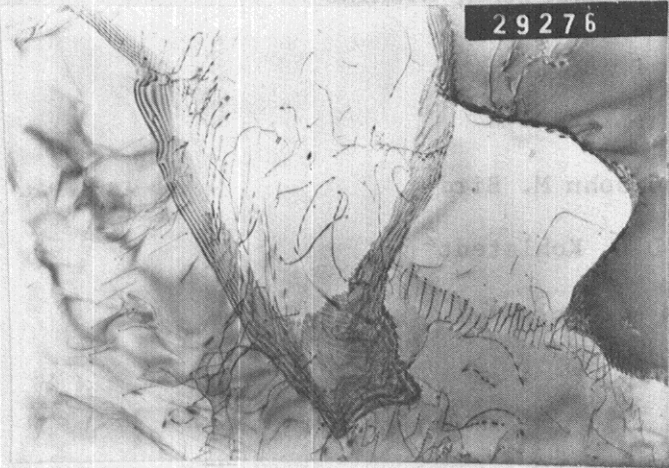
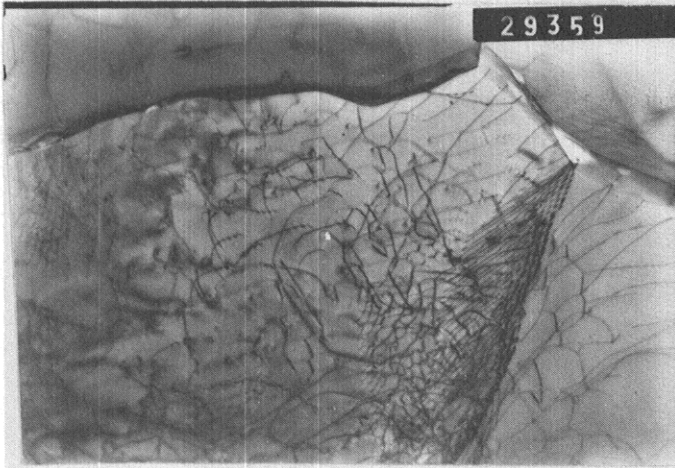
C

0.1 mm



D

1 mm



2  $\mu$ m

Department of Materials Science  
University  
New York 10023